

FATIGUE BEHAVIOUR OF POWDER STEEL SPECIMENS MADE BY SELECTIVE LASER MELTING

POKLUDA Jaroslav^{1,2}, HORNÍKOVÁ Jana², PÍŠKA Miroslav², ŠANDERA Pavel²

¹Alexander Dubček University of Trenčín, Trenčín, Slovak Republic, EU

²Brno University of Technology, Brno, Czech Republic, EU

Abstract

The Selective Laser Melting (SLM) is an advanced technology of producing three-dimensional solid objects by 3D printing from a digital file. The article deals with fatigue push-pull testing of SLM samples to determine the dependence of their fatigue characteristics on the orientation of laser melted layers to the loading axis, the hatch spacing of the laser beam and the surface roughness of 3D printed objects. The results revealed that the transverse orientation of layers (90° to the loading axis) led to a defect type of fracture and to a lower fatigue life than that exhibited by both the horizontal (0°) and inclined (45°) orientations. The standard hatch spacing led to a higher fatigue life than the reduced one. The samples with machined and polished surfaces revealed, due to their very small averaged surface roughness, a much better fatigue resistance than that exhibited by the as-built specimens.

Keywords: Selective laser melting, fatigue properties, layer orientation, surface roughness

1. INTRODUCTION

The production of 3D printed objects is achieved using additive processes in which the object is built by laying down successive layers of material until the entire object is created. The material quality depends on the technology how the particles are brought and joined together in the fusion. The state of the fusion is crucial because the solid material (particles) are passing from solid state to the melted state and finally again into the solid state. Laser or electron beams are used as the power sources for metals [1, 2]. Machining of the materials is used as a standard technology improving the precision and quality of the sintered part. The properties and the extent of the surface layer depend on the process of plastic deformation, fracture and friction. In the case of SLM, an influence of the sintered material structure, the surface deformation and subsurface strain associated with individual material grains during the cutting process is also important [3].

While many studies have been carried out to investigate the influence of surface treatment on the mechanical properties and fatigue resistance of wrought and cast engineering materials and components, a significantly less number of similar studies was devoted to SLM fabricated parts. In some works, for example, the effect of SLM process parameters on microstructure and basic mechanical properties, surface quality and machinability of the stainless steel 316L was studied [4, 5]. This article aims to present results concerning the dependence of fatigue resistance on the orientation of laser melted layers to the loading axis, the hatch spacing of the laser beam and the quality of the surface of 3D printed objects made of the powder ultra-high strength die steel MARLOK® C1650. Although not all sintered surfaces can be finished by polishing, knowledge of surface and microstructural integrity is very important for high demanding parts like medical implants or aeronautical parts where the surface quality is a crucial factor.

2. MATERIAL, FABRICATION AND FATIGUE TESTS

The MARLOK® C1650 is a powder ultra-high strength die steel of very low carbon and increased N, Mo and Co contents. The size distribution of grains of the MARLOK® powder (**Figure 1**) was analysed by the electron beam microscope VEGA 3 TESCAN and program Particles. The mean grain size was of about 20 µm in

diameter. The system Concept Laser (SINTEF, Trondheim) was used for fabrication of all specimens. This SLM device was equipped with an Nd:YAG laser which produced the laser beam with a wavelength of 1064 nm in the continuous horizontal scanning mode. The spot diameter of the laser beam 15 μm was set in the range of 5 to 200 μm and the scan laser velocity was 600 mm/s. The specimens were fabricated with two different hatch spacings of the laser beam: the standard $h_s = 0.1050$ mm and the reduced $h_r = 0.0525$ mm. Three different orientations in the building chamber were prepared: horizontal ($\alpha = 0^\circ$), inclined ($\alpha = 45^\circ$) and transverse ($\alpha = 90^\circ$) - see **Figure 2**.

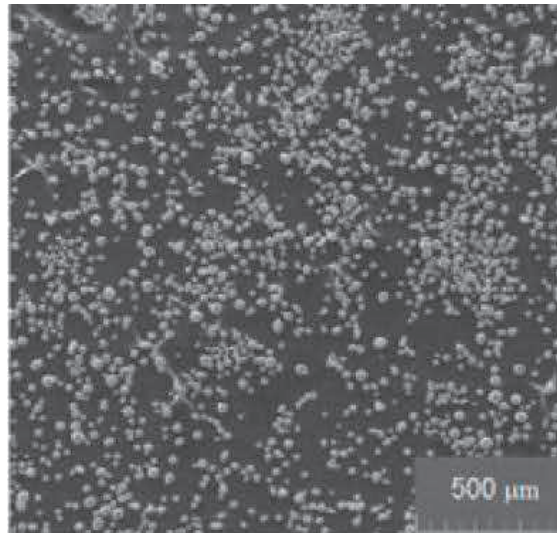


Figure 1 Microstructure of the MARLOK® C1650 powder ultra-high strength steel

Table 1 An overview of polished and as-built specimens and their markings

	Polished samples												As-built samples							
Hatch spacing	0.1050						0.0525						0.1050			0.0525				
Orientation	0°			45°			90°			0°			45°			0°				
Marking of samples	A1	A2	A3	B1	B2	B3	C1	C2	D1	D2	D3	E1	E2	E3	F1	F2	F3	G1	G2	G3

The CNC machining was done using the turning centre SPN 12 and the Sinumerik 840D control system. Rounded cutting inserted ISCAR GIMY 315-UN IC8250, tool holder TGDL 2525-3M and a special chuck for precise clamping and support. Cutting speed was of 100 m / min, feed per revolution of 0.02 mm and a shallow depth of cuts of 0.2 mm and an intensive outer cooling was done with emulsion CIMCOOL CIMSTAR 597. After turning, all samples were ground with abrasive belts of 400 and 600 μm grit grade and polished with a fine felt and diamond pastes Struers of grain size 5.0, 2.0, 1.0, 0.25 μm to get a glossy appearance. An overview of markings of such fabricated specimens along with those as-built (without any surface treatment) is displayed in **Table 1**.

The surface quality of each sample was investigated with the Alicona Infinite Focus G4 microscope prior to the fatigue testing. The 3D pictures of the surface topology were constructed and the surface roughness R_a (the arithmetic average of microscopic peaks and valleys) was determined.

The servohydraulic dynamic testing machine Instron 8874 was used for fatigue loading of samples by harmonic cycles with the frequency of 0.2 Hz in the push-pull regime (cyclic ratio $R = -1$). Three different nominal stress amplitudes $\sigma_a = 589, 668$ and 756 MPa were applied in each series of samples A, B, D, E F and G. Only two amplitudes $\sigma_a = 589$ and 756 MPa were employed in the case of C specimens due to their defect fracture behaviour.

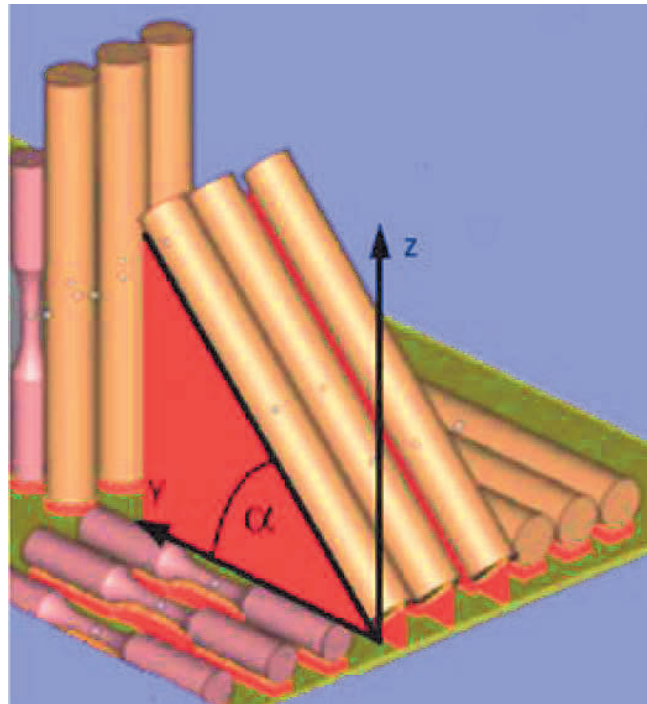


Figure 2 Orientation of the SLM samples

3. RESULTS AND DISCUSSION

Examples of 3D surface topography of polished and as-built samples are depicted in **Figure 3**. The surface of the polished specimens with standard hatch spacing exhibited a very smooth topology ($R_a = 0.2 \mu\text{m}$) - see **Figure 3a**. The polished specimens with reduced hatch spacing revealed a higher surface roughness, typically $R_a = 0.6 \mu\text{m}$. On the other hand, the roughness of as-built specimens with standard hatch spacing F3 was much higher, typically $R_a = 2.6 \mu\text{m}$ - see **Figure 3b**. The roughness of as-built specimens with reduced hatch spacing could even reach $R_a = 18 \mu\text{m}$.

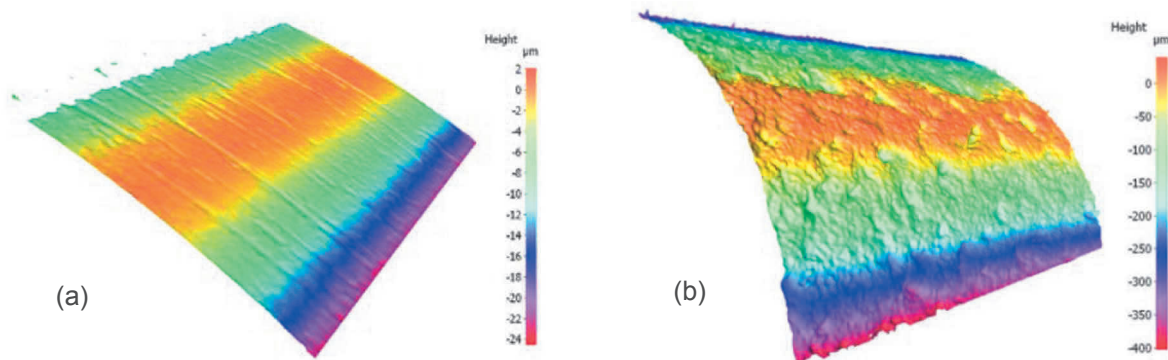


Figure 3 Surface topology of (a) specimen A1; (b) specimen F3

Fatigue data of all investigated samples are summarized in **Table 2** in terms of the applied stress amplitude σ_a and the number of cycles to fracture N_f and the related S-N curves are plotted in **Figure 4**. There is no significant difference in fatigue resistance of polished samples A and B with horizontal ($\alpha = 0^\circ$) and inclined ($\alpha = 45^\circ$) orientation, respectively. The same holds for the polished samples D and E. Thus, only two S-N curves for polished samples with standard (A+B) and reduced (D+E) hatch spacing are displayed in **Figure 4**. One can see that the fatigue resistance of the A+B samples is better than that of the D+E ones. This

corresponds to the fact that the averaged surface roughness of the A+B specimens was smaller than that of the D+E ones. Only one S-N curve for as-built specimens (F+G) is plotted in **Figure 4** since the difference in fatigue life between the as-built samples with standard and reduced hatch spacing was negligible (within the scatter range). Fatigue resistance of these specimens is much lower than that of the polished ones which also well corresponds to a very high surface roughness of as-built samples. Indeed, the surface was a highly preferential crack initiation site of all A, B, C, D, E, F and G specimens - see **Figure 5a**.

Table 2 Fatigue resistance of investigated specimens

	Applied stress amplitude σ_a [MPa]	Number of cycles to fracture N_f
A1	756	16 704
A2	668	21 892
A3	589	37 988
B1	756	6 065
B2	668	22 530
B3	589	13 357
C1	756	6 860
C2	668	108
D1	756	5 283
D2	668	10 739
D3	589	12 177
E1	756	6 150
E2	668	2 950
E3	589	19 600
F1	756	2 382
F2	668	3 477
F3	589	3 938
G1	756	1 795
G2	668	3 077
G3	589	8 026

On the other hand, the fatigue life of polished samples C with the transverse orientation was very small and the fracture occurred in between the clamping jaws (outside the measured length). The fracture surfaces of these specimens exhibited a defect morphology consisting of smooth intergranular facets indicating decohesion between non-sintered particles - see **Figure 5b**. This indicated that the crack initiation sites were in the specimen bulk at the intergranular pores and along the overlapping laser tracks (inter-layer bands), here oriented perpendicular to the direction of applied load.

The averaged values of fatigue life N_f for specimens A+B (polished, standard), D+E (polished, reduced) and F+G (as-built) can also be plotted without any reference to the applied stress amplitude as shown in **Figure 6**. Here the differences between the averaged fatigue life of individual types of samples are even more evident than it was in **Figure 4**.

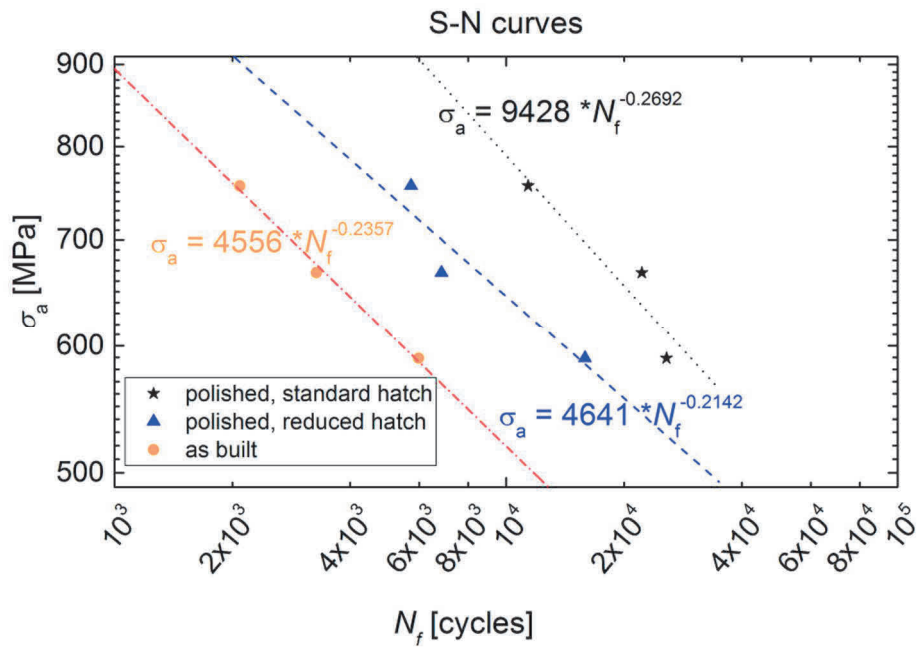


Figure 4 S-N curves for polished and as-built specimens

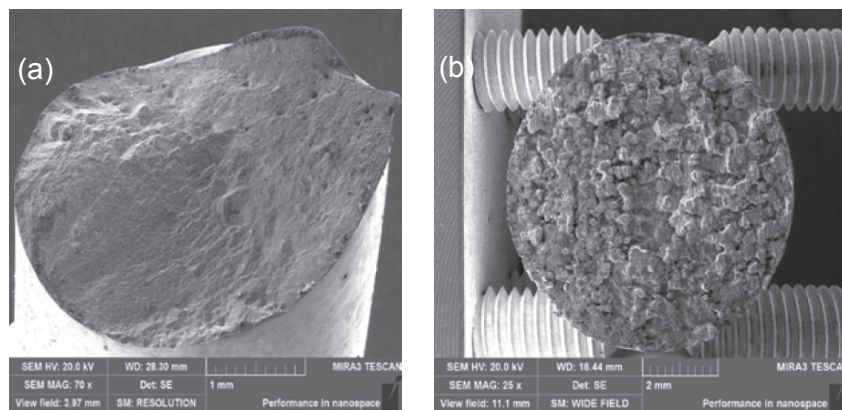


Figure 5 Fracture surface of (a) specimen A2, crack initiated at the surface (left bottom); (b) specimen C2

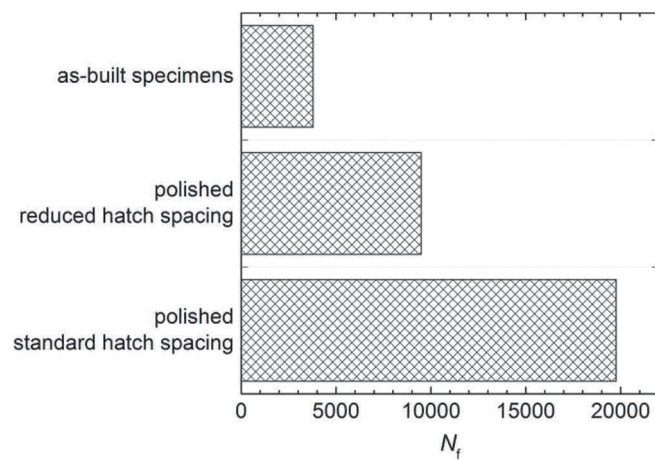


Figure 6 Averaged values of fatigue life N_f for polished and as-built specimens without any reference to the applied stress amplitude

4. CONCLUSIONS

The fatigue resistance of 3D printed objects made of the powder ultra-high strength steel MARLOK® C1650 to push-pull loading was studied in dependence on the orientation of laser melted layers to the loading axis, the hatch spacing of the laser beam and the quality of the surface. The main results of this analysis can be briefly summarized in the following points:

- (i) Machining and final polishing of samples with horizontal ($\alpha = 0^\circ$) and inclined ($\alpha = 45^\circ$) orientations led to a much better fatigue resistance than that revealed by the as-built samples without any surface treatment. Fatigue cracks in all these samples initiated on the specimen surface.
- (ii) There was no clear difference between the fatigue resistance of polished samples with horizontal (0°) and inclined (45°) orientations to the loading axis.
- (iii) The fatigue resistance of polished samples with the transverse ($\alpha = 90^\circ$) orientation was very small. The fatigue cracks initiated in the specimen bulk at intergranular pores and along overlapping laser tracks (inter-layer bands).
- (iv) The resistance of polished samples with horizontal (0°) and inclined (45°) orientations and standard hatch spacing was higher than that of the specimens with reduced hatch spacing. The reason could be found in a higher surface roughness of the latter specimens.

In general, the polishing of specimens led to a significant improvement of fatigue life. The polished samples with the standard hatch spacing exhibited the highest fatigue resistance. On the other hand, the fatigue life of polished specimens was substantially reduced by the transverse orientation of layers and the reduced hatch spacing.

ACKNOWLEDGEMENTS

This research was supported by the Slovak Research and Development Agency in the frame of the grant APVV-15-0710 and by the Specific University research of Brno University of Technology in the frame of the project FSI-S-17-4504.

REFERENCES

- [1] VAN DER EIJK, C., ÅSEBØ, O., MUGAAS, T., KARLSEN, R., SKJEVDAL, R., BOIVIE, K. Metal printing process: A rapid manufacturing process based on xerography using metal powders. *Materials Science and Technology*, 2005, vol. 3, pp. 3-9.
- [2] ZHU, Y., TIAN, X., LI, J., WANG, H. Microstructure evolution and layer bands of laser melting deposition Ti-6.5Al-3.5Mo-1.5Zr-0.3Si titanium alloy. *Journal of Alloys and Compounds*, 2014, vol. 616, pp. 468-474.
- [3] CASALINO, G., CAMPANELLI, S.L., CONTUZZI, N., LUDOVICO, A.D. Experimental investigation and statistical optimisation of the selective laser melting process of a maraging steel. *Optics & Laser Technology*, 2015, vol. 65, pp. 151-158.
- [4] CHERRY, J.A., DAVIES, H.M., MEHMOOD, S., LAVERY, N.P., BROWN, S.G.R., SIENZ, J. Investigation into the effect of process parameters on microstructural and physical properties of 316L stainless steel parts by selective laser melting. *International Journal Advanced Manufacturing Technology*, 2015, vol. 76, pp. 869-879.
- [5] TRUBAČOVÁ, P., PÍŠKA, M., HORNÍKOVÁ, J., ŠANDERA, P., SLÁMEČKA, K. Analysis of Selective Laser Melting Process Parameters Effect on Mechanical and Material Properties for Stainless Steel 316L. *Solid State Phenomena*, 2017, vol. 258, pp. 579 - 582.